Electronic Supplementary Material (ESI) for Physical Chemistry Chemical Physics.

Pt@TiO$_2$ Nanocomposite Electrocatalysts with Enhanced Methanol Oxidation by Hydrophobic Nanoreactor Templating

Supporting Information

*Tobias Unmüssig [a,b], Julia Melke[a,b], and Anna Fischer [a,b,c]**

* *corresponding author: anna.fischer@ac.uni-freiburg.de*

[a] Institute of Inorganic and Analytical Chemistry, University of Freiburg, Albertstraβe 21, 79104 Freiburg, Germany

[b] FMF – Freiburg Materials Research Center, University of Freiburg, Stefan-Meier-Straße 19, 79104 Freiburg, Germany

[c] FIT – Freiburg Center for Interactive Materials and Bioinspired Technologies, University of Freiburg, Georges-Köhler-Allee 105, 79110 Freiburg, Germany

Calculation of Theoretical Cell Voltage E^0_{cell}

$$2\ CH_3OH + 3\ O_2 \rightarrow 2\ CO_2 + 4\ H_2O \quad (E^0_{cell} = 1.19\ V) \tag{S1}$$

$$\Delta G^0 =- nFE^0_{cell} \tag{S2}$$

The theoretical cell voltage E^0_{cell} for methanol oxidation according to Equation (S1) is calculated from the change of Gibbs energy ΔG^0 based on Equation (S2). The other parameters in the equation are the number of transferred electrons $n = 6$ and the Faraday constant F =96485 C/mol. ΔG^0 is calculated according to Equation (S3). The standard reaction enthalpy ΔH^0 is calculated by the difference of the sum of the product and educt standard molar enthalpies of formation H^0_f (Equation (S4)). The standard reaction entropy ΔS^0 is calculated by the difference of the sum of the product and educt standard molar entropies S^0 (Equation (S5)).

$$\Delta G^0 = \Delta H^0 - T\Delta S^0 \tag{S3}$$

$$\Delta H^0 = \sum H^0_{f,Products} - \sum H^0_{f,Educts} \tag{S4}$$

$$\Delta S^0 = \sum S^0_{Products} - \sum S^0_{Educts} \tag{S5}$$

The standard molar enthalpies of formation and standard molar entropies for the products end educts of methanol oxidation to CO_2 according to Equation (S1) are listed in Table S1. From this, the theoretical cell voltage E^0_{cell} can be calculated to $E^0_{cell} = 1.19$ V at $T = 298.15$ K if all products and educts are in gaseous state.

Table S1: Standard molar enthalpies of formation and standard molar entropies at 298.15 K for the products and educts of methanol oxidation.[1]

Compound	**H^0_f in kJ/mol**	**S^0 in J/mol*K**
CH_3OH	-201 (aq:-239.2)	239.9 (aq: 126.8)
O_2	0	205.2
CO_2	-393.5	213.8
H_2O	-241.8 (aq:-285.8)	188.8 (aq: 70)

EDX Quantification of loaded PS_{111}-*b*-$P4VP_{96}$ micelles and Pt@TiO_2

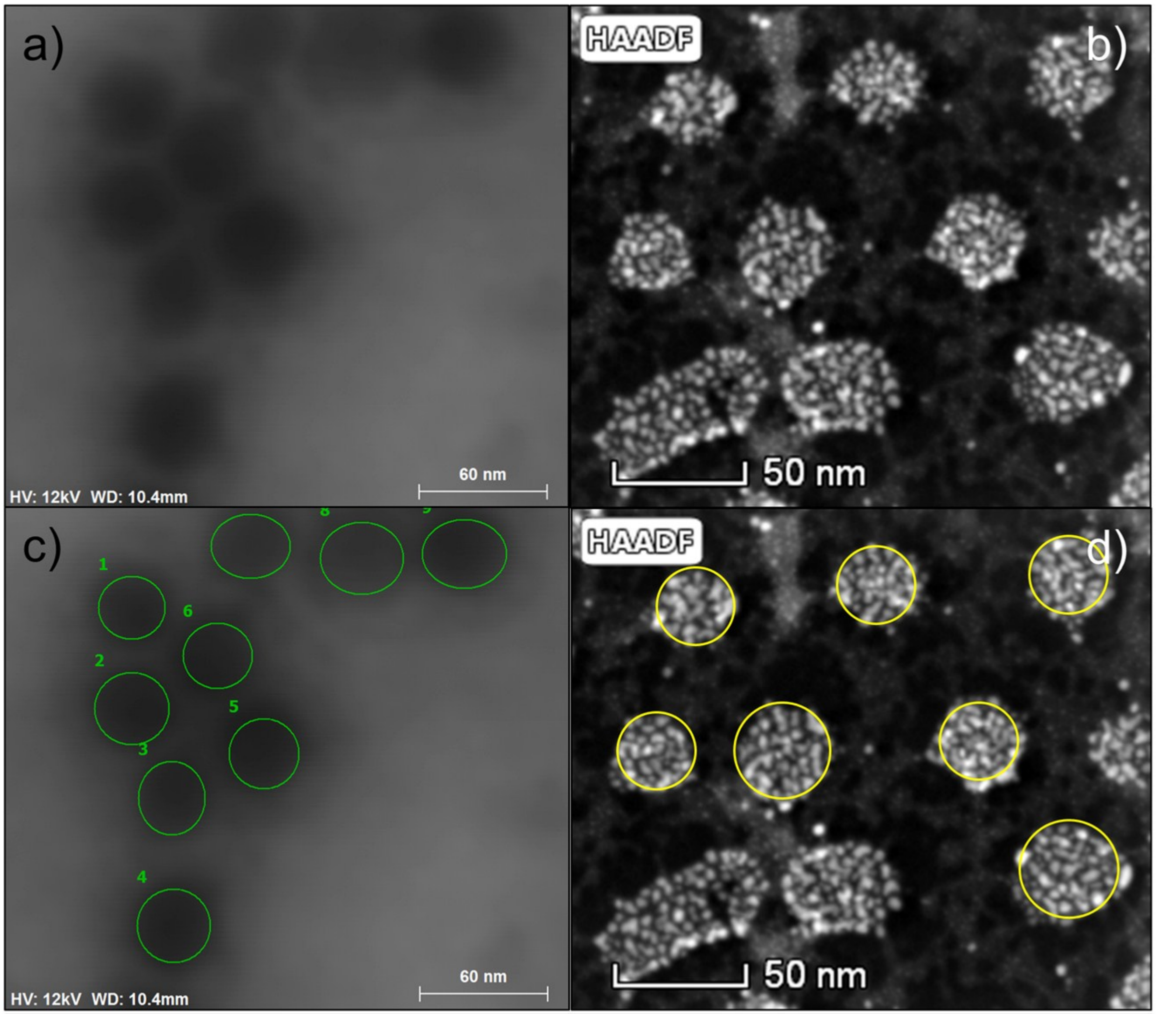

e)	$TiCl_4$/H_2PtCl_6·$6H_2O$@PS_{111}-*b*-$P4VP_{96}$	Pt@TiO_2
Atomic ratio (Ti:Pt)	1.78 ± 0.16	1.76 ± 0.13
Mass ratio (Ti:Pt)	0.44 ± 0.04	0.46 ± 0.03

Figure S1: STEM micrograph of PS_{111}-*b*-$P4VP_{96}$ micelles after loading with $TiCl_4$ and H_2PtCl_6·$6H_2O$ (a,c). HAADF-STEM micrograph of Pt@TiO_2 structures after calcination at 500 °C under air and reduction at 400 °C in 10 vol.% H_2 in N_2 (b,d). Comparison of Ti:Pt atomic ratio and mass ratio based on the EDX quantification (e). The circles in the micrographs mark the regions, which were used for EDX quantification.

STEM Characterization of $Pt@TiO_2$

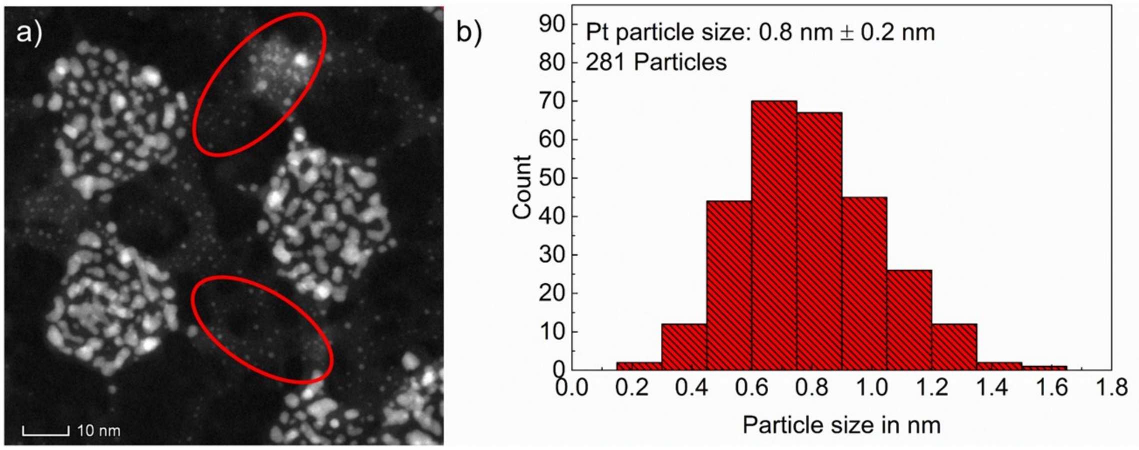

Figure S2: HR-STEM micrograph of $Pt@TiO_2$ nanocomposites after calcination at 500 °C under air and reduction at 400 °C in 10 vol.% H_2 in N_2. The red markings show the small platinum nanoparticles in the space between the $Pt@TiO_2$ structures (a). Particle size distribution of the small platinum nanoparticles in the space between the $Pt@TiO_2$ structures (b).

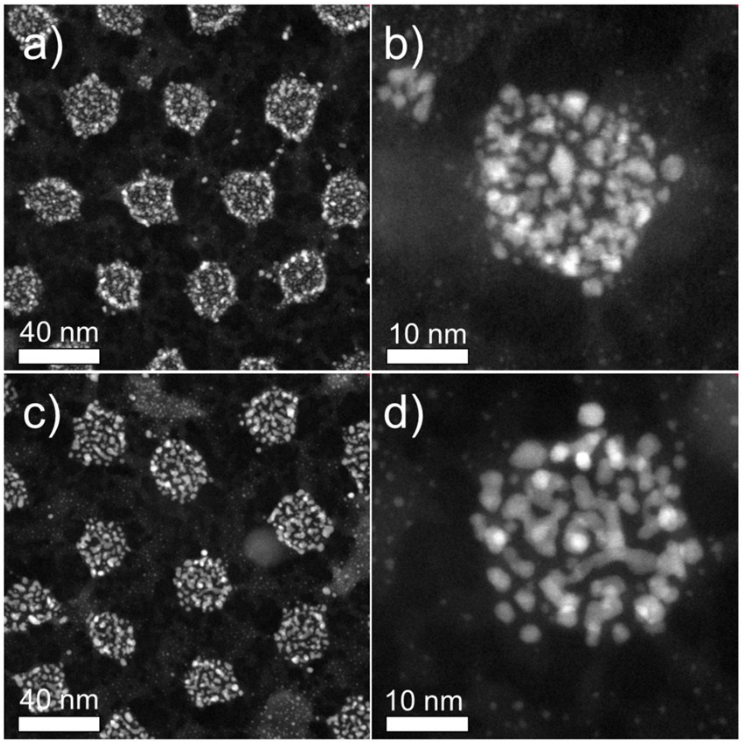

Figure S3: HR-STEM micrographs of $Pt@TiO_2$ nanocomposites after calcination at 500 °C under air (a,b) and subsequent reduction at 400 °C in 10 vol.% H_2 in N_2 (c,d).

HAADF-STEM Characterization of Pt/XC72

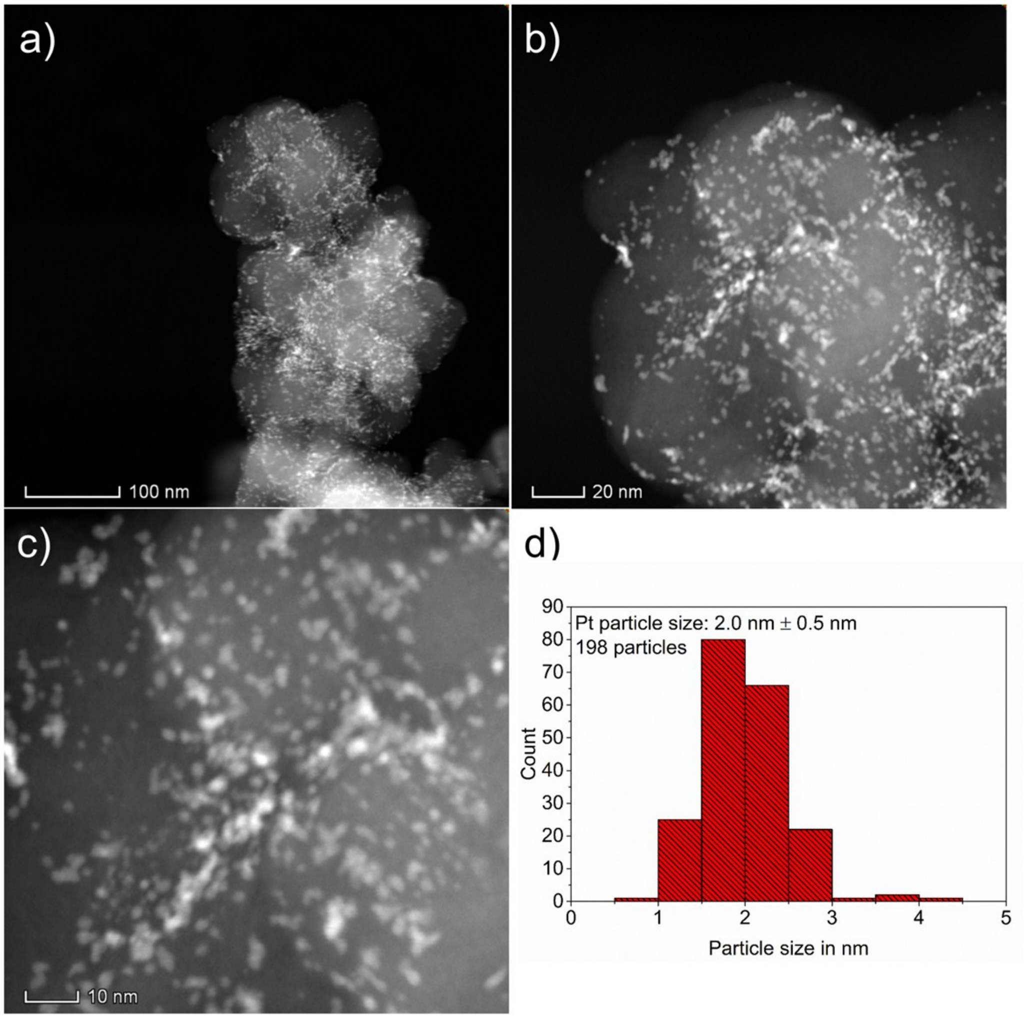

Figure S4: HAADF-STEM micrographs of the Pt/XC72 reference catalyst (a-c). Particle size distribution of the platinum nanoparticles (d).

XPS results of Pt@TiO_2 and Pt/XC72

Table S2: Binding energies, full width at half maximum (FWHM) and relative intensities of the different platinum species from the Pt4f XPS signal of Pt@TiO_2 and Pt/XC72.

Material	Species	Binding energies of Pt4f$_{7/2}$ (eV)	FWHM (eV)	Relative intensities (%)
Pt@TiO_2	Pt^0	70.9	1.3	89.6
	Pt^{2+}	72.3	1.3	7.4
	Pt^{4+}	73.5	1.3	3
Pt/XC72	Pt^0	71.7	1.6	77.3
	Pt^{2+}	73.7	1.8	16.2
	Pt^{4+}	75.4	1.8	6.5

Table S3: Binding energies and FWHM of Ti^{4+} species from the Ti2p XPS signal of Pt@TiO_2. No Ti^{3+} species were detected.

Material	Peak	Binding energy of Ti^{4+} (eV)	FWHM (eV)
Pt@TiO_2	Ti2p$_{3/2}$	458.8	1.4
	Ti2p$_{1/2}$	464.5	2.2

XPS of Pt-NA

Figure S5 (a) shows a platinum nanoarray (Pt-NA) on ITO coated glass, which was processed in the same way like the Pt@TiO_2 nanocomposites with the exception that no $TiCl_4$ was used in the synthesis. After dip-coating on ITO coated glass, the sample was calcined at 500 °C under air, followed by reduction at 400 °C in 10 vol.% H_2 in N_2. Figure S5 (b) shows the XPS measurement of the Pt4f signal and the peak deconvolution of Pt-NA on a silicon wafer. Based on the fitting result, platinum is only present as Pt^0 (98.4 at.%) with a binding energy of 71.2 eV.

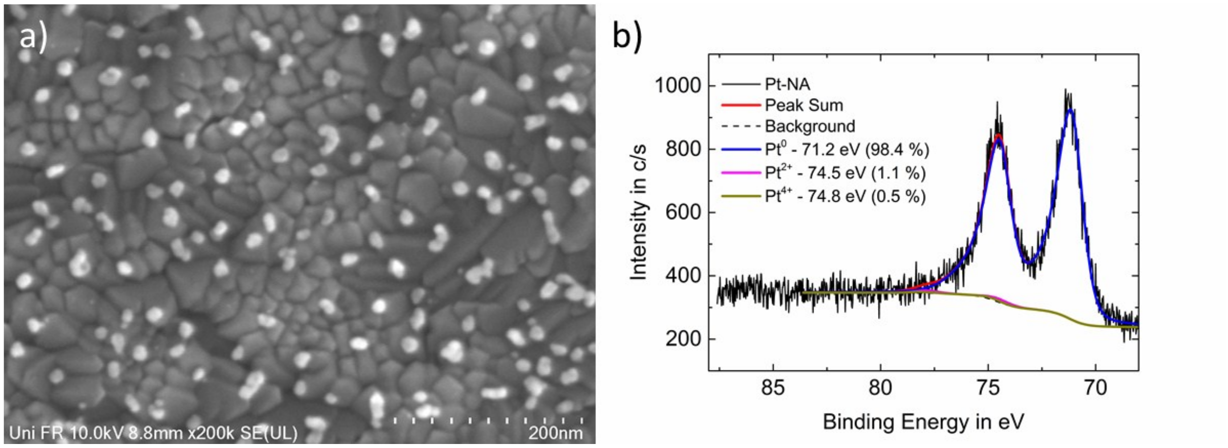

Figure S5: HR-SEM micrograph of Pt-NA on ITO coated glass after calcination at 500 °C under air and reduction at 400 °C in 10 vol.% H_2 in N_2 (a). XPS measurement and peak deconvolution of the Pt4f signal of Pt-NA on a silicon wafer after calcination at 500 °C under air and reduction at 400 °C in 10 vol.% H_2 in N_2 (b).

Pt@TiO$_2$ on ITO coated glass

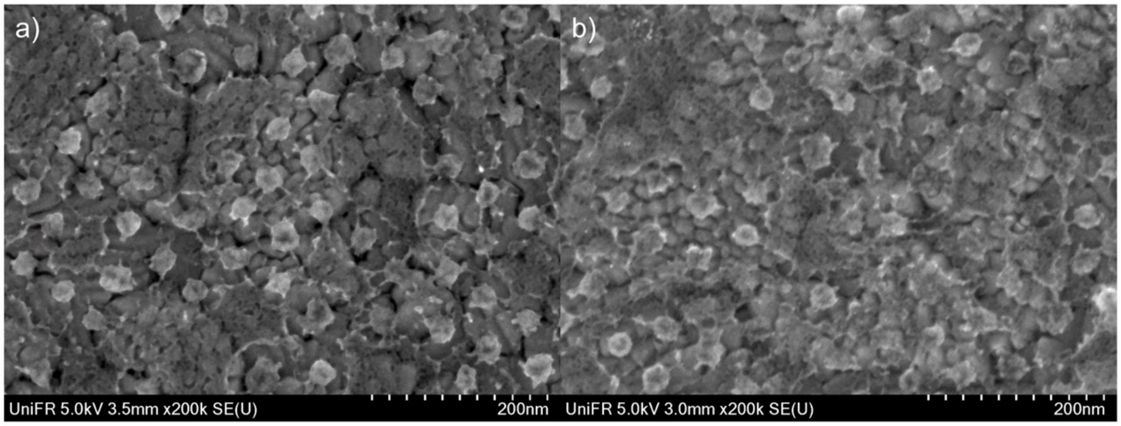

Figure S6: HR-SEM micrographs of Pt@TiO$_2$ structures coated as monolayers on ITO coated glass after calcination at 500 °C under air and reduction in 10 vol.% H$_2$ in N$_2$: as-synthesized (a), after electrochemical measurements (Conditioning: 0.03-1.2 V vs. RHE, 0.1 M HClO$_4$, 200 cycles; Methanol oxidation: 0.03-1.2 V vs. RHE, 0.1 M HClO$_4$ + 1 M MeOH, 20 cycles (b).

Mechanism of formic acid and formaldehyde oxidation

Similar as for the oxidation of methanol on platinum, a dual-pathway mechanism is proposed for formic acid and formaldehyde oxidation.[2–4] A non-CO pathway, leading to weakly adsorbed intermediates, and the CO-pathway leading to strongly adsorbed CO.[2,4]

In case of formic acid the non-CO pathway leads to formate ($HCOO^-$) as shown in Equation (S6) and (S7).[2,3] The CO pathway is shown in equation (S8), which then proceeds further as mentioned for methanol oxidation in Equation (6).

$$HCOOH + Pt \rightarrow Pt\text{-}HCOO + H^+ + e^- \qquad \text{(S6)}$$

$$Pt\text{-}HCOO \rightarrow Pt + CO_2 + H^+ + e^- \qquad \text{(S7)}$$

$$HCOOH + Pt \rightarrow Pt\text{-}CO + H_2O \qquad \text{(S8)}$$

In case of formaldehyde, which is hydrated to methylene glycol in aqueous solution (Equation (S9)), formate is a possible intermediate for the non-CO pathway (Equation (S10) and (S11).[4] As mentioned for methanol and formic acid oxidation, there is a CO-pathway as shown in Equation (S12).

$$HCOH + H_2O \rightarrow H_2C(OH)_2 \qquad \text{(S9)}$$

$$H_2C(OH)_2 \rightarrow Pt\text{-}HCOO + 3\ H^+ + 3\ e^- \qquad \text{(S10)}$$

$$Pt\text{-}HCOO \rightarrow Pt + CO_2 + H^+ + e^- \qquad \text{(S11)}$$

$$H_2C(OH)_2 \rightarrow Pt\text{-}CO + H_2O + 2\ H^+ + 2\ e^- \qquad \text{(S12)}$$

REFERENCES

[1] D. R. Lide, *CRC Handbook of Chemistry and Physics*, CRC Press, Boca Raton, **2008**.

[2] E. Gyenge, in *PEM Fuel Cell Electrocatal. Catal. Layers* (Ed.: J. Zhang), Springer, London, **2008**, pp. 165–270.

[3] H. Okamoto, W. Kon, Y. Mukouyama, *J. Phys. Chem. B* **2005**, *109*, 15659–15666.

[4] A. Miki, S. Ye, T. Senzaki, M. Osawa, *J. Electroanal. Chem.* **2004**, *563*, 23–31.